Regular Article

PHYSICAL CHEMISTRY RESEARCH
Published by the
Iranian Chemical Society
www.physchemres.org
info@physchemres.org

Phys. Chem. Res., Vol. 10, No. 2, 251-265, June 2022
DOI: 10.22036/PCR.2021.293370.1933

Kinetic Analysis of Hydrolytic Decomposition of Rubrocurcumin Analogues

J. John[a,b], S.D. Rugmini[b] and B.S. Nair[b,c,*]

[a]*Department of Chemistry, Christian College, Kattakada, University of Kerala, Thiruvananthapuram*
[b]*Department of Chemistry, Mahatma Gandhi College, University of Kerala, Thiruvananthapuram*
[c]*Principal, NSS College Ottapalam, Kerala, Thiruvananthapuram*

(Received 3 July 2021, Accepted 15 November 2021)

Rubrocurcumin, the spiroborate complex of curcumin and oxalic acid, is classically used in the microscale estimation of boron in soil and plant samples. However, alternate methods are suggested due to its low hydrolytic stability in water-mediated conditions. For hydrolysis, the precursors for the preparation of the complex-curcumin, oxalic acid and boric acid, are generated and thus can be used for the release of curcumin, the super antioxidant. The decomposition kinetics of rubrocurcumin and its analogues were studied in the aqueous-organic medium at different temperatures and pH values by monitoring the absorption peaks of the complex at its wavelength maxima. The decomposition products were identified using UV-Vis and ^{11}B NMR spectroscopy. The hydrolysis reaction was catalyzed by OH- ions and our results showed that these complexes were more stable at lower pH. A plausible mechanism for the hydrolysis of rubrocurcumin is proposed.

Keywords: Curcumin, Spiroborate complex, The mechanism for the hydrolysis, Decomposition kinetics, Hydrolytic stability

INTRODUCTION

Rubrocurcumin, chemically known as 1,3,2-dioxaborines, [2-{[1,7-bis(4-hydroxy-3-methoxyphenyl)-5-oxohepta-1,3,6-trien-3-yl]oxy}-1,3,2-dioxaborolane-4,5-dione] is the spiroborate ester formed from the condensation reaction of curcumin, boric acid, and oxalic acid [1-2] (Fig. 1). They have been found to be more thermally stable than curcumin [3-4]. Resembling transition metal complexes of curcumin [5], rubrocurcumin and its analogues retain their antioxidant properties; however, this retention is slightly less than that of curcumin [6]. Rubrocurcumin is a biologically active compound and is highly active against HIV proteases [2]. Rubrocurcumin is more biostable than natural curcumin in physiological medium and possess more efficacies for anti-cancer activity compared with curcumin and is a suggested candidate for site targeted drug delivery [7]. A recent study showed that Beta Tri Calcium Phosphate

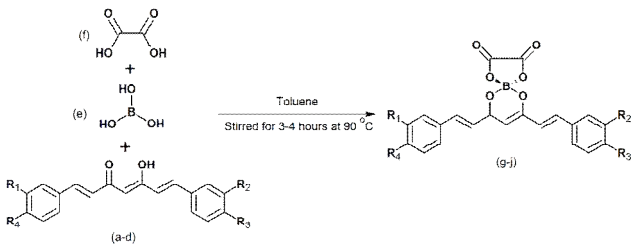

Fig. 1. Synthesis of rubrocurcumin analogues from different curcumin analogues.
(a-CC: R_1=R_2=OCH_3, R_3=R_4=OH; b-DMC: R_1=H, R_2=OCH_3, R_3=R_4=OH; c-BDMC: R_1=R_2=H, R_3=R_4=OH; d-DHCC: R_1=R_2=R_3=R_4=H; e-Boric acid; f-Oxalic acid; g-CBO 1: R_1=R_2=OCH_3, R_3=R_4=OH; h-CBO 2: R_1= H, R_2=OCH_3, R_3=R_4=OH; i-CBO 3: R_1=R_2=H, R_3=R_4=OH; j-CBO 4: R_1=R_2=R_3=R_4=H)

(β-TCP) and Hydroxyapatite/Beta Tri Calcium Phosphate (HA-βTCP) incorporated with nanoparticles of spiroborate ester of curcumin with maleic acid can serve as biostable

*Corresponding author. E-mail: sbcnair@gmail.com

curcumin incorporated scaffold for sustained drug release and is a promising candidate for bone regeneration and repair owing to its inherent osseous properties [8]. Along with the antiproliferative property of rubrocurcumin, the boron present in rubrocurcumin helps in neutron capture therapy of tumor cells [9]. However, classically rubrocurcumin is known as the reddish complex soluble in alcoholic solution and used in the microscale determination of boron in various fields [10-11].

The precursor of rubrocurcumin, curcumin, is well known for its biological activity and is effective against various diseases like inflammation, infection, cancer, cataract, arthritis, diabetes, cardiovascular, neurological disorders, *etc*. [12-15]. The main crisis that restricts the use of curcumin as a therapeutic drug is its low bioavailability due to less aqueous solubility, rapid degradation in alkaline medium, poor absorption, rapid metabolism and elimination which results in the low curcumin concentration in tissues and blood [16-17]. A possible method to increase its bioavailability is to incorporate curcumin with some other carriers like liposomes, phospholipids, microparticles or nanoparticles which can be converted back to curcumin when required [18-21]. Curcumin metal complexes are better carriers [22-23] and curcumin boron complexes are principally suitable because of their low hydrolytic stability [24].

Considering the applications of spiroborate esters of curcumin, detailed knowledge on the hydrolytic stability of rubrocurcumin and their analogues is essential. Curcumin extracted from the rhizome of the plant turmeric contains three closely related species: Curcumin (CC), Demethoxy Curcumin (DMC), and Bisdemethoxy Curcumin (BDMC), which differ only in the number of methoxy groups presented in the compound [25]. All these yellow-colored pigments are known for various biological properties with different grading. In its classical application, estimation of boron, the formation of rubrocurcumin and its decomposition at different rates create issues regarding standardization, especially when curcumin from different varieties of turmeric is used containing different compositions of these pigments. The ability of rubrocurcumin to release curcumin in various physiological and aqueous conditions makes it an interesting candidate for selective curcumin delivery. An understanding of the hydrolytic stability of rubrocurcumin analogue is important to evaluate its efficiency as a curcumin release drug.

The hydrolysis of curcumin in different reaction conditions was well studied along with various factors that affect its hydrolytic stability such as pH, temperature, light, metal ions, oxygen levels, and antioxidants [26-32]. Stability studies on curcumin are important because its stability affects the physiological properties of curcumin. The effect of pH is prominent among these factors and curcumin easily undergoes degradation under neutral-basic conditions. In acidic conditions, only 20% of curcumin degrades within 1 hour and in basic pH, more than 90% of curcumin degrades within 30 min [29]. The degradation of curcumin follows second-order kinetics in the methanol-water system to form ferulic acid and feruloylmethane as initial hydrolysis product followed by the hydrolysis of feruloylmethane to produce vanillin and acetone as final products [26].

In the present study, rubrocurcumin and its three analogues were synthesized using CC, DMC, BDMC, and DHCC (curcumin analogue with no substituent in the benzene ring, Figure 1d) and were named CBO 1, CBO 2, CBO 3, and CBO 4, respectively (Fig. 1). The hydrolytic stabilities of these four analogues were carried out and the influence of factors such as solvent, temperature, and pH on the rate of hydrolysis was studied and a reasonable mechanism was suggested.

EXPERIMENTAL

Materials

Acetone, acetonitrile, acetic acid, methanoland1, 4-dioxane purchased from Spectra Chem., Mumbai served as solvents and was further purified by the methods reported in the literature [33]. CC and DMC were separated chromatographically from commercial curcumin [5] and used for the preparation of CBO 1 and CBO 2. BDMC [due to low percentage in commercial sample] and DHCC were synthetically prepared by the method reported in the literature and used for the preparation of CBO 3 and CBO 4 [34].

Methods

UV-Vis absorption spectra of compounds were recorded

in acetonitrile solution (10^{-6} M) using Elico 198 Biospectrophotometer fitted with a quartz cuvette of 1 cm path length within the range of 200-700 nm. IR spectra were recorded using PerkinElmer IR spectrophotometer using KBr disc. ^{1}H NMR spectra were recorded on Bruker Avance NMR spectrometer using DMSO as solvent. Chemical shifts are reported in ppm using tetramethylsilane as the internal standard. ^{13}C NMR spectra were recorded on Bruker Avance NMR spectrometer using DMSO-d_6 as solvent. Chemical shifts are reported in ppm using the solvent resonance as the internal standard (DMSO-39.5 ppm).

The stock solution of CBO analogues (≈10^{-3} M) was prepared in acetone, acetonitrile, acetic acid, methanol, and 1,4-dioxane solvents. Except for methanol solution, all other stock solutions were found to be stable at ambient temperature. In methanol solvent, slow degradation was observed and thus kept at a subzero temperature, and fresh stocks were prepared for each batch of studies. The aqueous organic solvent mixtures were prepared in double distilled water prepared in a glass water distiller. For kinetic measurements, the concentration of the CBO analogue was kept at 10^{-5} M. The aqueous organic solvent mixtures were prepared in a 100 ml standard flask by adding corresponding volumes of organic solvents and double distilled water using a burette.

For the hydrolysis product analysis, UV-Vis spectrophotometer and ^{11}B NMR spectrometer were used. ^{11}B NMR spectra were recorded on 160 MHz Bruker Avance NMR spectrometer using DMSO as solvent and pyrex glass as the standard (d=0), and the chemical shifts were recorded in ppm.

Hydrolytic Stability of CBO Analogues in Aqueous Acetone

The stability of CBO analogues in an aqueous organic medium was monitored by measuring the decrease in the absorbance at their wavelength maxima using thermostated UV-Vis spectrophotometer (Elico 198 Biospectrophotometer with Peltier assembly). The reducing peak at 540 nm was selected for the kinetic studies since the product peak undergoes variation due to the further decomposition of curcumin.

The first-order rate constant for degradation was obtained from linear regression analysis of the logarithm of the concentration of CBO analogue against time, and also using the integrated equation for first order reaction (Eq. (1)), where "a" is the initial concentration and "a-x" is the concentration at any time, t [35]. All studies were carried out in duplicate.

$$k = \frac{2.33}{t}\log\frac{a}{a-x} \tag{1}$$

The influence of solvent on the rate of hydrolysis of CBO analogues was determined in different organic solvent systems prepared by mixing desired volumes of organic solvents and distilled water. The solvent influence was analyzed using the linear free energy relationship; Grunwald-Winstein (GW) equation (Eq. (2)), which is widely used to study the influence of solvent on the rate of solvolysis reaction [36-37].

$$\log\left(\frac{k}{k_0}\right) = mY_x \tag{2}$$

Where k and k_0 are the rate constants in the solvent concerned and 80% ethanol-water system, and m is the sensitivity to changes in solvent ionizing power Y, originally obtained by taking tert-butyl chloride as the standard (m = 1).

The effect of temperature on the rate of hydrolysis was investigated by carrying out the reaction at five different temperatures (40 to 60 °C). Activation energy and Arrhenius frequency factor for the hydrolysis reaction were calculated using the Arrhenius equation (Eq. (3)) [38-39],

$$\log k = \log A - \frac{E_a}{2.303\,RT} \tag{3}$$

Where k is the rate constant, A is the Arrhenius frequency factor, E_a is the activation energy, R is the universal gas constant, and T is the reaction temperature. From the slope and intercept of the straight-line plot logk *vs.* 1/T, the magnitude of E_a and A was determined. The Eyring equation (Eq. (4)) was used to calculate the values of enthalpy and entropy of activation [38,40-41].

$$\ln\frac{k}{T} = \frac{\Delta H^{\neq}}{RT} + \ln\frac{k_B}{h} + \frac{\Delta S^{\neq}}{R} \tag{4}$$

In above formulation, k_B and h are the Boltzmann and Planks constant, respectively. From the slope and intercept of Eyring plot ln(k/T) *vs*. 1/T, $\Delta H^{\#}$ and $\Delta S^{\#}$ were calculated. The equation $\Delta G^{\#} = \Delta H^{\#} - T\Delta S^{\#}$ was used for the calculation of free energy of activation [41].

The hydrolysis of CBO analogues under various pH conditions ranging from 4-9 was investigated in a 50% acetone water system using different buffer solutions. Acetate buffer was used for acidic pH (4-6), and phosphate buffer was used for basic pH (7-8). Sodium carbonate-sodium bicarbonate buffer was used for the preparation of pH 9 [42].

Data Analysis

Microsoft Office Excel worksheet was used for performing data analysis. The correlation coefficient and standard deviation were used for checking the validity of experimental results.

RESULTS AND DISCUSSION

Stability of CBO Analogues in Aqueous Organic Medium

The UV-Vis spectrum of CBO analogues in an aqueous organic medium (Fig. S1, supplementary information) showed a continuous decrease in absorbance at its λ_{max} region with time, and dropped to almost zero absorbance at infinite time, which indicates complete hydrolysis. For all CBO analogues, along with the decrease in peak at λ_{max} region, an increase of peak at 420 nm with time was obtained. The absorbance at the wavelength of about 475 nm was constant through the reaction; that absorbance value is called isobestic point. This occurs because the two substances absorb light of that specific wavelength to the same extent, and the analytical concentration remains constant. At 475, a clear isosbestic point was observed, which shows that the two principal species presented in the system are the reactant, CBO 1 with λ_{max} value at 540 nm, and the product, curcumin with λ_{max} value at 420 nm in acetone.

However, the rate of increase in peak at 420 nm diminished with time and finally, resulted in a decrease in peak due to the decomposition of formed curcumin [26,29].

Effect of Substituents on the Hydrolytic Stability of CBO Analogues

The hydrolytic rate data of CBO analogues in different percentages of the acetone-water system is presented in Table 1. The rate of hydrolysis increased with an increase in water percentage for all CBO analogues. As the concentration of organic solvent increased, CBO analogues which were soluble in organic solvents were surrounded by numerous solvent molecules and the availability of aqueous reagents decreased, which resulted in enhanced hydrophobic interaction of substrate and organic solvents [43]. The trend for hydrolysis rate constant of CBO analogues in 50% acetone water system is CBO 4 > CBO 1 > CBO 2 > CBO 3 and thus the hydrolytic stability order is CBO 3 > CBO 2 > CBO 1 > CBO 4. CBO 4, with no substituent in the benzene ring, had the highest rate constant and showed the least stability in water-mediated conditions. The highest stability i.e. lowest rate constant was observed for the CBO 3 formed from BDMC which have a *p*-OH substituent in both benzene rings. If a carbocation or a partially positive charged center is formed during the reaction, as suggested in the reaction of dioxaborine dyes [44], the presence of a

Table 1. Hydrolysis Rate Data for CBO Analogues in Different % of the Acetone-water System at 50 °C

% Of acetone	Mole fraction of acetone	10^5 k (s^{-1})			
		CBO 1	CBO 2	CBO 3	CBO 4
20	0.057	12.23 ± 0.04	12.29 ± 0.04	11.95 ± 0.03	24.17 ± 0.06
30	0.095	6.32 ± 0.03	6.62 ± 0.02	6.33 ± 0.02	16.09 ± 0.03
40	0.140	3.32 ± 0.03	2.64 ± 0.02	2.34 ± 0.02	8.50 ± 0.03
50	0.196	1.76 ± 0.01	1.32 ± 0.01	0.94 ± 0.01	4.68 ± 0.02
60	0.268	1.05 ± 0.01	0.61 ± 0.01	0.43 ± 0.01	2.88 ± 0.02

strong electron donating hydroxyl group will increase the rate of reaction by stabilizing the carbocation center in the transition state, and the *m*-methoxy group presented in CBO 2 and CBO 1 enhances the influence of the hydroxyl group to a lesser extent. CBO 4, devoid of –OH and $–OCH_3$ showed the highest rate constant k_1 which ruled out the possibility of a carbocation intermediate formation during hydrolysis. The decrease rate constant with the hydroxyl substitution supports the formation of a negatively charged transition state. However, an increase in k_1 value with $-OCH_3$ substitution discards this possibility. As seen from the order of hydrolysis rate, the number of methoxy groups led to a decrease in the hydrolysis rate. CBO 2, formed from demethoxycurcumin, can form a strong intramolecular hydrogen bond with the corresponding *p*-OH group [45]. CBO 1 formed from curcumin can form two intramolecular hydrogen bonds with both *p*-OH substituents. Except CBO 2, all other CBO analogues are symmetric in nature and differ only in the extent of the hydrogen bond formed. The intramolecular hydrogen bonding of the methoxy group was changed with the concentration of water in the solvent system and formed intermolecular hydrogen bonding interaction with the solvent. These interactions explain the reason for variation in antioxidant properties of curcumin and the curcuminoids [46]. The present authors also reported that the variation of this hydrogen bonding interaction played a major role in the thermal stability of rubrocurcumin analogues [47].

Effect of Solvent on the Rate of Hydrolysis

The first-order rate constant k_1 observed in the hydrolysis of CBO analogues in aqueous organic solvents namely acetonitrile, acetic acid, 1,4-dioxane, and methanol were similar to that of acetone and are presented in Tables S1-4, and the corresponding plots are given in Figs. S2-6 (supplementary information). It can be observed that the effect of the percentage of water is slightly different for different CBO analogues. The hydrolysis rate decreased in the order methanol > acetic acid > acetonitrile > acetone > dioxane in 40% aqueous organic media. Faster hydrolysis took place in protic solvents, however, a lower rate constant was observed for acetic acid due to its acidic pH. Among the non-protic solvent, the hydrolysis rate decreased with the decrease in solvent polarity. Similar to the case of curcumin, the rubrocurcumin analogues were stable in organic medium and extend of hydrolysis increased with an increase in the percentage of water. The influence of the percentage of water in solvents of different polarities was different for each analogue as shown in Figs. S2-5. At mole fraction 0.10 in acetone water mixture, CBO 1-3 showed the same rate and reversed rate profile was observed above and below this percentage. However, such a coinciding point was not observed for acetonitrile solution, even at 0.35 mol fraction. Yet, CBO 4 converges with other analogues at lower mole fractions. In dioxane, the convergence points were different for different analogues CBO 1-2 at 0.9, CBO 2-3 at 0.5, and CBO 1-3 at 0.11; CBO 4 converged with other analogues at lower mole fraction less than 0.6 as in the case of acetonitrile. In the acetic acid medium, the rate constants showed the same behavior for all the analogues. In methanol, instantaneous hydrolysis took place for CBO 4 and convergence points were not distinguishable within the studied mole fractions.

At a higher percentage of water, the intramolecular hydrogen bond between methoxy and hydroxyl groups diminished due to the strong intermolecular hydrogen bond formation with solvent water, and an increase in the rate of hydrolysis was observed. The effect was lower for CBO 2 than CBO 1, where the intramolecular hydrogen bond formation was only half, and for CBO 3 there is no intramolecular hydrogen bonding. The highest rate of CBO 3 below the mole fraction of acetone 0.116 explains the importance of solvent-substrate hydrogen bond interaction on the hydrolysis of CBO analogues and also on the antioxidant property of curcumin [48]. At the mole fraction of 0.116 of acetone, all CBO analogues had similar stability, and above this mole fraction, the rate increase was reversed. CBO 4, devoid of intramolecular hydrogen bonding, did not show any reversal in the rate at different percentages of water as in other CBO analogues. The stability variation of formed CBO analogues in different water percentages may be the cause of changes observed in the boron estimation when samples of different curcumin were used for estimation.

In polar protic solvents, methanol and acetic acid, water-solvent hydrogen bonding was more prominent than the water-substrate or methanol-substrate hydrogen bonding. Therefore, the influence of hydrogen bonding due to the

–OH and -OCH_3 groups on the reaction rate is negligible. In acetic acid, CBO 1-3 showed a similar rate and CBO 4, having no substituent in the benzene ring, showed better stability than the others. In the methanol-water system, CBO 1 and CBO 3 showed similar trends in hydrolysis rate with the variation of water percentage and were more stable than CBO 2. In the acetonitrile-water system, the influence of hydrogen bond was similar to acetone case; however, higher polarity made more significant influence among the CBO's. In the dioxane-water medium, the influence was comparatively smaller.

The rate data given in Table S1 (supplementary information) shows that for CBO 1, hydrolysis in protic polar methanol medium is only ten times faster than that in aprotic nonpolar acetone or dioxane with the same percentage of water content. A similar trend was observed for CBO 2-4 in the rate of hydrolysis according to solvent polarity (Tables S2-S4, supplementary information). The very small solvent effect in the hydrolysis of CBO analogues suggests the possibility of a chargeless intermediate where the initial and transition state have similar charge distribution *i.e.* possibility of an isopolar transition state during the hydrolysis. The GW plots with Y values based on tert-butyl chloride [49,50] for aqueous acetone for all CBO analogues are given in Fig. 2, and different solvents for each CBO are given in Fig. 3. The statistical data obtained from these GW plots are given in Table S5 (supplementary information) and summarized for CBO 1-4 in Tables S6-S9 (supplementary information).

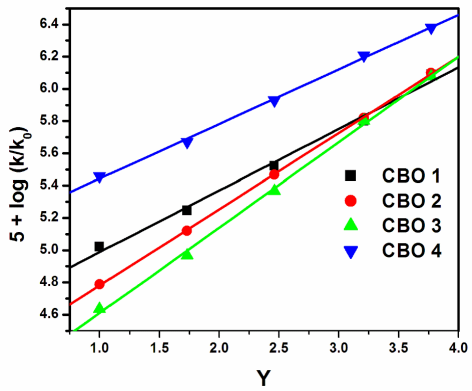

Fig. 2. GW plots for the hydrolysis of CBO analogues in aqueous acetone medium at 50 °C.

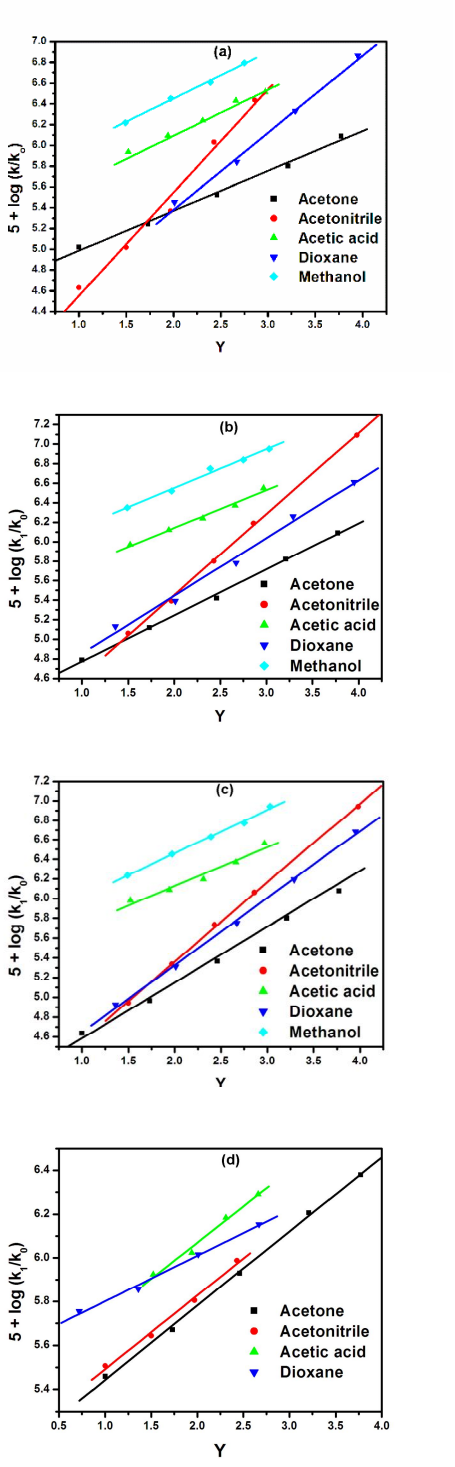

Fig. 3. GW plots for the hydrolysis of CBO analogues in different solvents at 50 °C (a) CBO 1 (b) CBO 2 (c) CBO 3 (d) CBO 4.

The GW plots exhibit a dispersion effect instead of a single correlation curve, with different linear plots for each solvent. The variation of intermolecular hydrogen bonding of substrate with water and co-solvent along with water co-solvent hydrogen bonding influenced the intramolecular hydrogen bonding [51-53]. A similar effect was reported in the antioxidant property of curcumin in different solvents by sequential proton loss electron transfer (SPLET) mechanism [54-55].

For a substitution reaction, the magnitude of m values is used as a criterion for the prediction of the mechanism. If the m value is > 0.7, it indicates a unimolecular elimination-addition pathway, and if m value is < 0.5, it indicates on bimolecular pathway [56]. The slope values obtained for all CBO analogues in different aqueous organic reaction mediums are summarized in Table 2. The slope values are quite different for each solvent and it follows the order acetonitrile > dioxane > methanol > acetic acid > acetone, for all CBO analogues.

For CBO 4, the m value for all the four solvents was about 0.33, with a slightly lower value of 0.21 in dioxane. The m values of protic solvents methanol and acetic acid had comparable values for all CBO analogues, which were in the range of 0.34-0.44 for methanol and in the range of 0.33-0.41 for acetic acid. However, the aprotic solvents behaved differently, especially, for dioxane and acetonitrile in which a large reduction in m value was observed for CBO 1 to CBO 4. In a polar protic medium, water and co-organic solvent can have hydrogen bond interaction with the substrate as well as one another. Due to strong co-solvent-water hydrogen bond interaction, substrate solvent hydrogen bond interactions are not prominent. But in a polar aprotic solvent that has weak hydrogen bond interaction with co-solvent and water, the substrate solvent interaction becomes important and the solvent effect has more influence on the nature of the reaction.

Effect of Temperature on the Rate of Hydrolysis

The first-order rate constants for the hydrolysis of CBO analogues in 50% acetone water solvent system at five different temperatures are recorded in Table 3, the corresponding Arrhenius plots show good linearity having a

Table 2. Slope Values of all CBO Analogues in Different Solvents

CBO analogues	Slope value obtained from GW plot				
	Acetone	Acetonitrile	Acetic acid	Dioxane	Methanol
CBO 1	0.3815	0.9919	0.4136	0.7345	0.4491
CBO 2	0.4704	0.8300	0.3880	0.5929	0.3931
CBO 3	0.5296	0.8039	0.3940	0.6812	0.4474
CBO 4	0.3389	0.3365	0.3320	0.2087	0.3389

Table 3. Hydrolysis Rate Data for CBO Analogues in 50% Acetone Water System at Different Temperatures Ranging from 40-60 °C

Temperature (°C)	$10^5 k_1$ (s^{-1})			
	CBO 1	CBO 2	CBO 3	CBO 4
40	0.48 ± 0.01	0.44 ± 0.00	0.38 ± 0.01	2.04 ± 0.02
45	1.03 ± 0.01	0.73 ± 0.02	0.67 ± 0.02	3.16 ± 0.01
50	1.76 ± 0.01	1.32 ± 0.01	0.94 ± 0.00	4.68 ± 0.01
55	2.95 ± 0.02	1.86 ± 0.01	1.72 ± 0.01	6.83 ± 0.02
60	4.45 ± 0.01	3.82 ± 0.01	2.87 ± .02	10.69 ± 0.01

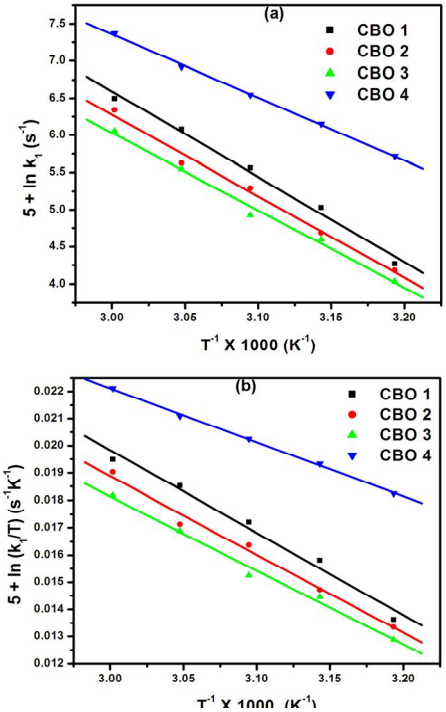

Fig. 4. (a) Arrhenius plots and (b) Eyring plots for the hydrolysis of CBO analogues.

negative slope with correlation coefficient 0.9944 to 0.9994, and standard deviation (SD) 0.1053 to 0.0258 (Fig. 4a). The $\Delta H^{\#}$ and $\Delta S^{\#}$ values were calculated from the slope and intercept of the linear Eyring plots (Fig. 4b), and are presented in Table 4.

The rate of hydrolysis at 25 °C is in the same order of magnitude despite the presence of different substituents in the benzene ring. The negligible substituent effect suggests that the site of the attack is not at the curcumin part and the slight variation in rate may be due to the difference in hydrogen bonding with substituent presented in different curcuminoids. There was a regular decrease of $\Delta H^{\neq}$ and an increase of $\Delta S^{\neq}$ from CBO 1-4. However, $\Delta G^{\#}$ was constant for CBO 1-3 with a slight decrease for CBO 4. The large positive $\Delta H^{\neq}$ and negative $\Delta S^{\neq}$ indicates the possibility of a bulky transition state [57]. $\Delta S^{\neq}$ varied significantly among the CBO analogues. For ion-dipolar type reaction, $\Delta S^{\neq}$ should nearly be the same which ruled out the possibility of an ion-dipolar type reaction. The free energy of activation $\Delta G^{\#}$ and activation energy E_a was in comparable order of magnitude, which suggests that the mechanism of hydrolysis of all these compounds should be similar. The large frequency factor of the order of 10^{33} to 10^{48} suggests that the reacting species are rather larger in size [58,59].

The isokinetic plot $\Delta H^{\neq}$ *vs.* $\Delta S^{\neq}$ given in Fig. 5a, is a linear plot with a correlation coefficient of 0.9982 showing that there is enthalpy entropy compensation [60]. The calculated isokinetic temperature β obtained from the slope of this plot is 369 K. The isokinetic temperature obtained from the slope of the Exner plot (Fig. 5b) was 357 K, where a log-log plot at two different temperatures was utilized (SD = 0.0295; R^2 = 0.9992; slope = 0.8489) [61]. The linear Exner plot suggests all CBO analogues undergo the same mechanistic path for the hydrolysis reaction. For an isoentropic reaction, β is infinity, and for an isoenthalpic reaction, it is zero [62]. The obtained isokinetic temperature implies that the hydrolysis reaction is neither isoenthalpic nor isoentropic, but obeys the compensation law.

Effect of pH on the Rate of Hydrolysis

CBO analogues can be hydrolyzed by H_2O, H_3O^+ or OH^- ions depending on the pH of the medium. A regular increase in the rate constant k_1 was observed with an

Table 4. Kinetic Parameters Calculated for the Hydrolysis of CBO Analogues at Different Temperatures

Compound	K_1 at 25 (°C s^{-1})	*Ea* (kJ mol^{-1})	*A* (s^{-1})	$\Delta H^{\neq}$ (kJ mol^{-1})	$-\Delta S^{\neq}$ (J K^{-1} mol^{-1})	$\Delta G^{\#}$ (kJ mol^{-1})	SD	R^2
CBO 1	8.42×10^{-7}	95.50	1.36×10^{44}	93.02	49.23	107.69	0.0955	0.9955
CBO 2	7.50×10^{-7}	90.77	3.97×10^{48}	88.29	66.04	107.98	0.0990	0.9947
CBO 3	7.04×10^{-7}	86.55	9.71×10^{38}	84.07	80.73	108.14	0.0811	0.9961
CBO 4	5.17×10^{-6}	70.85	8.21×10^{33}	68.38	116.77	103.19	0.0260	0.9994

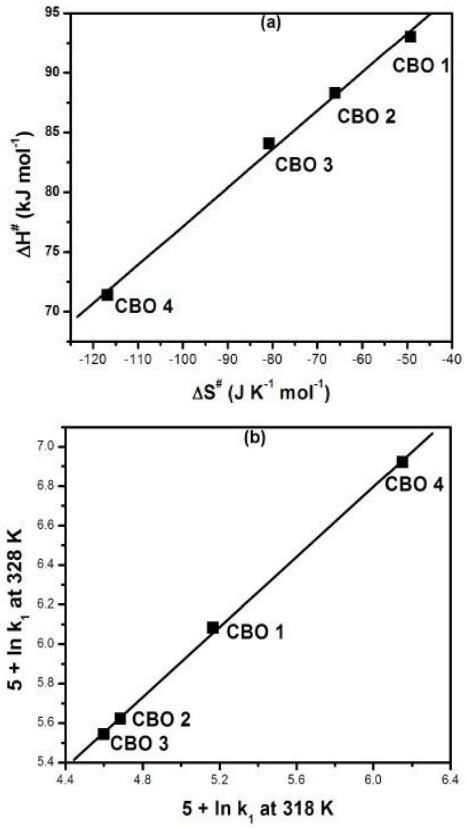

Fig. 5. (a) Isokinetic and (b) Exner plots for the hydrolysis of CBO analogues.

increase in the pH for all CBO analogues, as shown in Table 5, similar to the degradation kinetics of curcumin [26,29]. Recently, the present authors reported a similar increase in the rate constant with pH for the hydrolysis of rosocyanin, the 2:1 complex of curcumin with boric acid [24]. The influence of pH differs in CBO analogues. The unsubstituted analogue, CBO 4, showed the largest increase in the rate constant with an increase in pH values, approximately 7.5 time increase for a pH change from 4 to 6. The tremendous increase in hydrolysis with an increase in pH makes it impossible to study the hydrolysis rate at still higher pH. The influence of pH was minimal for CBO 1, where the hydrogen bond played a major role in rate constant values. At lower pH, all compounds showed the lower rate constant values, and these values converged for CBO 1-3, indicating that the intramolecular hydrogen bonds were intact. The presence of substituent in benzene ring,

Table 5. pH Dependence of Rate Constant for the Hydrolysis of CBO Analogues at 50 °C in 50% Aqueous Acetone

	$10^5 k_1$ (s^{-1})			
pH	CBO 1	CBO 2	CBO 3	CBO 4
4	1.24 ± 0.02	1.63 ± 0.01	1.27 ±0.02	5.56 ± 0.03
5	1.53 ± 0.01	7.92 ± 0.03	2.95 ±0.02	27.3 ± 0.04
6	5.52 ± 0.03	24.58 ±0.05	20.14 ±0.04	41.24 ±0.05
7	11.89 ±0.02	45.06 ±0.07	59.19 ±0.06	-
8	26.58 ±0.04	46.26 ±0.06	64.23 ±0.08	-
9	32.85 ±0.06	-	-	-

-OH as well as -OCH_3, led to a decrease in the hydrolysis rate with an increase in pH. At neutral and alkaline pH, the intermolecular hydrogen bonding with solvent water played a major role in determination of the mechanism of the reaction.

The Mechanism for the Hydrolysis of CBO Analogues

^{11}B NMR spectrum of rubrocurcumin (CBO 1) was studied at different time intervals during the hydrolysis reaction and the spectrum obtained during the hydrolysis reaction is given in Fig. 6. The sharp signals of the sample solution were superimposed by a very broad signal which originates from the glass of the sample tube, however, the signals of our interest were not affected by the broad signal. One high-frequency signal at 22.52 ppm and one low-frequency signal at 8.46 ppm can be seen in the spectrum. The resonance signal at 8.46 ppm may be assigned to the tetrahedral boron atom in the original bis-chelate complex [63]. The peak at 22.52 ppm is due to trigonal boron atoms of boric acid resulting from the hydrolysis of the rubrocurcumin [64]. Usually, the peak corresponding to boric acid is obtained around 18 ppm. The chemical shift value is very much influenced by solvents, temperature, pH, and pressure [65]. So the higher chemical shift obtained may be due to the reaction conditions employed for doing

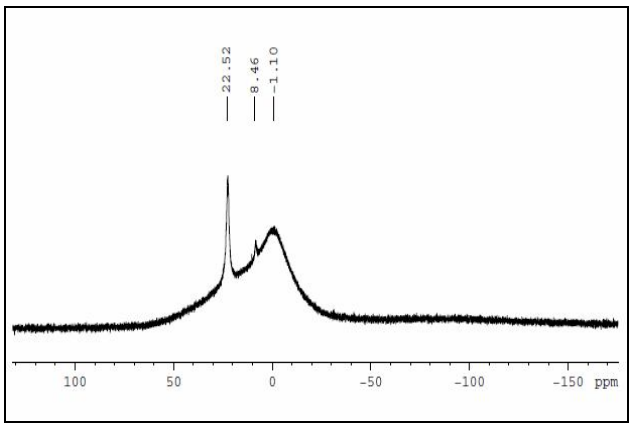

Fig. 6. ^{11}B NMR spectrum of CBO 1 obtained during hydrolysis.

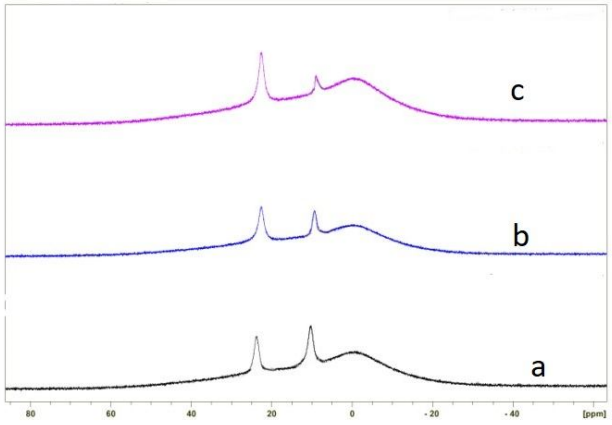

Fig. 7. ^{11}B NMR spectra of CBO 1 recorded during the hydrolysis in 50% acetone water system at room temperature. (a) After 1 h (b) after 5 h (c) after 10 h.

the hydrolysis reaction.

The combined ^{11}B NMR spectra for the hydrolysis of CBO 1 are presented in Fig. 7. The reduction of the peak at 8.46 ppm (Fig. 7) is due to the solvolysis of the pentagonal ring of boron in CBO, and the growth of the peak at 22.52 ppm is due to the formation of boric acid as the hydrolysis product [63]. UV-Vis spectra and ^{11}B NMR spectra confirmed that curcumin and [$B(OH)_3$] were the two hydrolysis products along with oxalic acid.

The involvement of the hydrogen-bonded water in the reaction and the formation of penta coordinated boron have

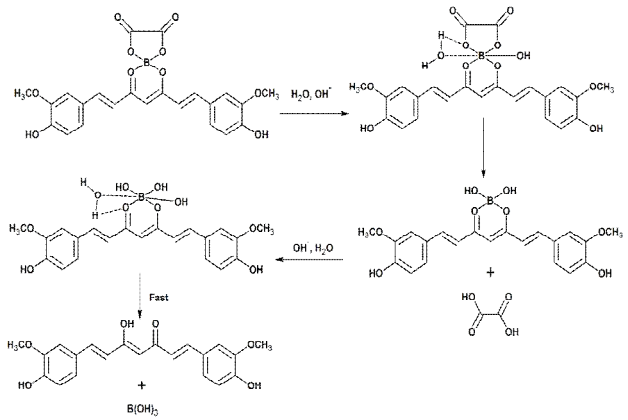

Fig. 8. Plausible mechanism for the hydrolysis of CBO 1.

been also predicated [66]. A two-stage decomposition is suggested for the base catalyzed hydrolysis of boron ester of chromotropic acid through the formation kinetics studies. In CBO analogues, boron is attached to two dissimilar rings and the site of attack resulting in the formation of the transition state, which is suggested to be away from the curcumin ring and closer to the lactone ring formed by the oxalic acid. The TG study results of CBO analogues reported the presence of hydrogen bonded water molecules in solid state and its absence in rosocyanin [24]. The mechanism for the hydrolysis reaction can be similar to that observed for rosocyanin and the salicylate derivative of rubrocurcumin, which can effectively explain the solvent effect and the enthalpy entropy compensation effects [24]. The proposed mechanism for the base catalyzed hydrolysis is depicted in Fig. 8.

In the basic condition, the hydroxyl group in the reaction medium attacks the tetrahedral boron atom to form a pentavalent boron species as a transition state. The boron atom and one of the oxygen atoms in the oxalate group presented in this transition state formed a hydrogen bond with water molecules. The hydrogen bonding is shown as dashed lines in Fig. 8. The formation of the transition state is a slow process and hence it determines the rate of the hydrolysis reaction. The formation of a charged less bulky transition state can be confirmed by the observed negligible solvent effect and high negative $\Delta S^{\#}$ values. Negligible substituent effect and enthalpy entropy compensation effect confirm that the reaction site is not on the curcumin side and

is on the other side of curcumin boron bonds. Accordingly, in the second step, the B-O bonds of oxalic acid ring break along with the OH bond of water molecule resulting in the formation of tetrahedral curcumin boron complex with two OH groups. Solvent effect studies and ^{11}B NMR studies gave clear indication regarding the formation of this intermediate as a hydrolysis product

If the curcumin part degrades first, then the product is curcumin and 1:1 boron oxalic acid complex. ^{11}B NMR spectra give a new peak for this compound. But no such peaks were observed in the ^{11}B NMR spectra (Fig. 7). This indicates that the oxalic acid part degrades first, which follows the degradation of the curcumin part. Another observation that substantiates the lactone ring breaking for rubrocurcumin is the less hydrolysis rate variation among the CBO analogues. If the ring ruptures on the curcumin side first, then the change in rate with the change in substituents in the curcumin ring may be higher. The third stage of the reaction is fast in which the second curcumin similarly undergoes hydrolysis to release curcumin and boric acid as remaining hydrolysis products. Since $\Delta G^{\#}$ and *Ea* values obtained for all CBO analogues are in the same order, all of them similarly undergo hydrolysis. The validity of isokinetic relation also indicates a similar hydrolysis mechanism for the CBO analogues.

CONCLUSIONS

Rubrocurcumin is nontoxic and found to have significant biological activities similar to curcumin. The oral intake of rubrocurcumin is a suggestive method especially in presence of oily food materials in which it is soluble as well as more stable. In the oral tract, the pH influence may partially hydrolyze rubrocurcumin, but the formed product was curcumin, the active drug. In the intestine, the low pH and less water mediated condition make rubrocurcumin more stable and the release of curcumin is slow. The constant curcumin concentration in the stomach may help with longer absorption of curcumin to bloodstream and this requires more studies to evaluate the bioavailability of rubrocurcumin and curcumin by the oral intake of rubrocurcumin. The rate and mechanism of CBO provide data on the curcumin release in different conditions. The hydrolysis of four CBO analogues followed first-order kinetics in all reaction mediums. As the percentage of water in the reaction medium increased, the rate of hydrolysis also increased, thus oily medium is more suggestive for better stability of rubrocurcumin. The solvent effect studies shed light upon the concerted reaction through the formation of an isopolar transition state. The increase in the rate of hydrolysis in the basic medium indicates the possibility of a base catalyzed reaction which suggests stable nature and slow hydrolysis rate of rubrocurcumin at lower pH and thereby slow release of curcumin. The mechanistic route suggested that the influence of substituents in the ring had less influence on the rate of reaction and it is not suggestive for stabilizing the compounds. The knowledge about the mechanism for the hydrolysis of CBO helps with increasing the validity of the curcumin method used for boron determination and using them as a carrier for curcumin in the human body.

SUPPLEMENTARY INFORMATION

Hydrolysis rate data and statistical data for the hydrolysis of CBO analogues in acetone water system obtained from GW plot are given in Tables S1 to S9. The UV-Vis spectrum of CBO 1 in 50% acetone water medium at 50 °C taken at a definite time interval during hydrolysis is given in Fig. S1.

ACKNOWLEDGEMENTS

The authors are thankful to the Sophisticated Analytical Instrument Facility (SAIF), Cochin University of Science and Technology and the Indian Institute of Science Education and Research, Trivandrum for carrying out the spectral analysis. One of the authors (JJ) is grateful to the Council of Scientific and Industrial Research for its financial support in the form of Senior Research Fellowship (08/538(0003)/2012-EMR-1).

REFERENCES

[1] Spicer, G. S.; Strickland, J. D. H., Compounds of curcumin and boric acid. Part II. The structure of rubrocurcumin. *J. Chem. Soc.* **1952**, *0*, 4650-53, DOI: 10.1039/JR9520004650.

[2] Sui, Z.; Salto, R.; Li, J.; Craik, C.; Ortiz de Montellano, P. R., Inhibition of the HIV-1 and HIV-2 proteases by curcumin and curcumin boron complexes, *Bioorg. Med. Chem.* **1993**, *1*, 415-22, DOI: 10.1016/s0968-0896(00)82152-5.

[3] John, J.; Sudha, D. R.; Balachandran, S., Effect of the substituent on the thermal stability of spiroborate esters of curcumin, *J. Therm. Anal. Colorim.* **2020**, *139*, 3537-47, DOI: 10.1007/s10973-019-08739-y.

[4] Daniel, A. B.; Aruldhas, D.; John, J.; Balachandran, S.; Joe, I. H., Molecular structure, vibrational spectra and density functional theory of the spiro-conjugated anticancer active molecule rubrocurcumin, *Spectroscopy Lett.*, **2020**, *53*, 12-31, DOI: 10.1080/00387010.2019.1690521.

[5] Priya, R. S.; Balachandran, S.; Daisy, J.; Mohan, P. V., Reactive centers of curcumin and the possible role of metal complexes of curcumin as antioxidants, *Univ. J. Phys. Appl.* **2015**, *3*, 6-16, DOI: 10.13189/ujpa.2015.030102.

[6] John, J.; Sudha, D. R.; Balachandran, S., A comparative study on the antioxidant properties of curcuminoids and its rubrocurcumin analogues, *Bull. Pure Appl. Sci.* **2018**, *37*, 121-25, DOI: 10.5958/2320-320X.2018.00016.X.

[7] Anjana, S.; Joseph, J.; John, J.; Balachandran, S.; Kumar, T. R. S.; Abraham, A., Novel flourescent spiroborate esters: potential therapeutic agents in *in vitro* cancer models, *Molec. Biol. Rep.* **2018**, *46*, 727-740, DOI: 10.1007/s11033-018-4529-5.

[8] Kumari, L. S.; Joseph, J.; John, J.; Pillai, R. S.; Balachandran, S.; John, A.; Abraham, A., Curcumin spiroborate ester incorporated hydroxyapatite-? tricalcium phosphate scaffolds for tissue engineering applications, *Trends Biomater. Artif. Organs.* **2018**, *32*, 97-104.

[9] Wang, S.; Blaha, C.; Santos, R.; Huynh, T.; Hayes, T. R.; Beckford-Vera, D. R.; Blecha, J. E.; Hong, A. S.; Fogarly, M.; Hope, T. A.; Raleigh, O.; Wilson, D. M.; Evans, M. J.; VanBrocklin, H. F.; Ozawa, T.; Flavell, R. R., Synthesis and initial biological evaluation of boron-containing prostate-specific membrane antigen ligands for treatment of prostate cancer using boron neutron capture therapy, *Mol. Pharmaceutics.* **2019**, *16*, 3831-41, DOI: 10.1016/B978-0-12-819460-7.00071-2.

[10] Farhat, A.; Ahmad, F.; Arafat, H., Analytical techniques for boron quantification supporting desalination processes: A review, *Desalination*, **2013**, *310*, 9-17, DOI: 10.1016/j.desal.2011.12.020.

[11] Liu, Y. M.; Lee, K., Modifications of the curcumin method enabling precise and accurate measurement of seawater boron concentration, *Mar. Chem.* **2009**, *115*, 110-17, DOI: 10.1016/j.marchem.2009.07.003.

[12] Liu, X. -F.; Hao, J. -L.; Xie, T.; Mukhtar, N. J.; Zhang, W.; Malik, T. H.; Lu, C. -W.; Zhou, D. -D., Curcumin, a potential therapeutic candidate for anterior segment eye diseases: A review, *Front. Pharmacol.* **2017**, *8*, 66, DOI: 10.3389/fphar.2017.00066.

[13] Nelson, K. M.; Dahlin, J. L.; Bisson, J.; Graham, J.; Pauli, G. F.; Walters, M. A., The essential medicinal chemistry of curcumin, *J. Med. Chem.* **2017**, *60*, 1620-37, DOI: 10.1021/acs.jmedchem.6b00975.

[14] Pulido-Moran, M.; Moreno-Fernandez.; Ramirez-Tortosa.; Ramirez-Tortosa, M., Curcumin and health, *Molecules*. **2016**, *21*, 264-86, DOI: 10.3390/molecules21030264.

[15] Sun, X.; Liu, Y.; Li, C.; Wang, X.; Zhu, R.; Liu, C.; Liu, H.; Wang, L.; Ma. R.; Fu, M.; Zhang, D.; Li, Y., *Biomed. Res. Int.* **2017**, *2017*, 1.

[16] Prasad, S.; Tyagi, A. K.; Aggarwal, B. A., Recent developments in delivery, bioavailability, absorption and metabolism of curcumin: the golden pigment from golden spice, *Cancer Res. Treat.* **2014**, *46*, 2-18, DOI: 10.4143/crt.2014.46.1.2.

[17] Anand, P.; Kunnumakkara, A. B.; Newman, R. A.; Aggarwal, B. B., Bioavailability of curcumin: problems and promises, *Mol. Pharm.* **2007**, *4*, 807-18, DOI: 10.1021/mp700113r.

[18] Asish, K. D.; Ikiki, E., Novel drug delivery systems to improve bioavailability of curcumin, *J. Bioequiv. Availab.* **2013**, *6*, 001, DOI: 10.4172/jbb.1000172.

[19] Madhavi, B. B.; Vennela, K. S.; Masana, P.; Madipoju, B., Enhanced transdermal drug penetration of curcumin via ethosomes, *Malays. J. Pharm. Sci.* **2013**, *11*, 48-58.

[20] Gao, M.; Chen, C.; Fan, A.; Zhang, J.; Kong, D.; Wang, Z.; Zhao, Y., Covalent and non-covalent curcumin loading in acid-responsive polymeric micellar nanocarriers, *Nanotechnology*. **2015**, *26*, 275101,

DOI: 10.1088/0957-4484/26/27/275101.

[21] Sherin, S.; Sheeja, S.; Sudha, D. R.; Balachandran, S.; Soumya, R. S.; Abraham, A., Curcumin incorporated titanium dioxide nanoparticles as MRI contrasting agent for early diagnosis of atherosclerosis-rat model, *Chem Biol. Interact.* **2017**, *275*, 35, DOI: 10.1016/j.vas.2020.100090.

[22] Renfrew, A. K., Transition metal complexes with bioactive ligands: mechanisms for selective ligand release and applications for drug delivery, *Metallomics*, **2014**, *6*, 1324-35, DOI: 10.1039/C4MT00069B.

[23] Renfrew, A. K.; Bryce, N. S.; Hambley, T. W., Delivery and release of curcumin by a hypoxia-activated cobalt chaperone: a XANES and FLIM study, *Chem. Sci.* **2013**, *4*, 3731-39, DOI: 10.1039/C3SC51530C.

[24] John, J.; Sudha, D. R.; Balachandran, S., Kinetics and mechanism of the thermal and hydrolytic decomposition reaction of rosocyanin, *Int. J. Chem. Kinet.* **2018**, *50*, 164-77, DOI: 10.1002/kin.21148.

[25] Song, W.; Qiao, X.; Liang, W. F.; Ji, S.; Yang, L.; Wang, Y.; Xu, Y. W.; Yang, Y.; Guo, D. A.; Ye, M., Efficient separation of curcumin, demethoxycurcumin, and bisdemethoxycurcumin from turmeric using supercritical fluid chromatography: From analytical to preparative scale, *J. Sep. Sci.* **2015**, *38*, 3450-53, DOI: 10.1002/jssc.201500686.

[26] Tonnesen, H. H.; Karlsen, J., Studies on curcumin and curcuminoids VI. Kinetics of curcumin degradation in aqueous solution, *Z Lebensm Unters Forsch*. **1985**, 180, 402-04, DOI: 10.1007/BF01027775.

[27] Tonnessen, H. H.; Karlsen, J.; Henegouwen, G. B., Studies on curcumin and curcuminoids. VIII. Photochemical stability of curcumin, *Z Lebensm Unters Forsch*, **1986**, *183*, 116-22, DOI: 10.1007/BF01041928.

[28] Tonnessen, H. H.; Masson, M.; Loftsson, T., Studies of curcumin and curcuminoids. XXVII. Cyclodextrin complexation: Solubility, chemical and photochemical stability, *Int. J. Pharm.* **2002**, *244*, 127-35, DOI: 10.1016/S0378-5173(02)00323-X.

[29] Wang, Y. J.; Pan, M. H.; Cheng, A. L.; Lin, L. I.; Ho, Y. S.; Hsieh, C. Y.; Lin, J. K., Stability of curcumin in buffer solutions and characterization of its degradation products, *J. Pharm. Biomed. Anal.* **1997**, *15*, 1867-76, DOI: 10.1016/s0731-7085(96)02024-9.

[30] Leung, M. H. M.; Mohan, P.; Pukala, T. L.; Scanlon, D. B.; Lincoln, S. F.; Kee, T. W., Reduction of copper(II) to copper(I) in the copper-curcumin complex induces decomposition of curcumin, *Aust. J. Chem.* **2012**, *65*, 490-95, DOI: 10.1071/CH12081.

[31] Hong, J., Curcumin-induced growth inhibitory effects on HeLa cells altered by antioxidant modulators, *Food Sci. Biotechnol.* **2007**, *16*, 1029-34.

[32] Masuda, T.; Hidaka, K.; Shinohara, A.; Maekawa, T.; Takeda, Y.; Yamaguchi, H. J., Chemical studies on antioxidant mechanism of curcuminoid: analysis of radical reaction products from curcumin, *Agric. Food Chem.* **1999**, *47*, 71-7, DOI: 10.1021/jf9805348.

[33] Furniss, B. S.; Hannaford, A. J.; Smith, P. W. J.; Tatchell, A. R., Vogel's Textbook of Practical Organic Chemistry, Dorling Kindersley (Ind) Pvt Ltd. (Pearson Education) **2006**, pp. 395-397.

[34] John, J.; Rugmini, S. D.; Balachandran, S., Kinetic analysis of thermal and hydrolytic decomposition of spiroborate ester of curcumin with salicylic acid, *Orient. J. Chem.* **2017**, *33*, 849-58, DOI: 10.13005/ojc/330234.

[35] Fathalla, M. F., Solvent effect on the alkaline hydrolysis of 2-thiophenyl-3,5-dinitropyridine, *Int.* J. *Chem. Kinet.* **2006**, *38*, 159-65, DOI: 10.1002/kin.20146.

[36] Grunwald, E.; Winstein, S., The correlation of solvolysis rates, *J. Am. Chem. Soc.* **1948**, *70*, 846-54, DOI: 10.1021/ja01182a117.

[37] Winstein, S.; Grunwald, E.; Jones, H. W., The correlation of solvolysis rates and the classification of solvolysis reactions into mechanistic categories, *J. Am. Chem. Soc.* **1951**, *73*, 2700-07, DOI: 10.1021/ja01150a078.

[38] Hindra, F.; Baik, O. D., Kinetics of quality changes during food frying, *Crit. Rev. Food Sci. Nutr.* **2006**, *46*, 239-58, DOI: 10.1080/10408690590957124.

[39] Veeken, A.; Hamelers, B., Effect of temperature on hydrolysis rates of selected biowaste components, *Bioresour. Technol.* **1999**, *69*, 249-54, DOI: 10.1016/S0960-8524(98)00188-6.

[40] Al-Ghouti, M.; Khraishehb, M. A. M.; Ahmada, M. N.

M.; Allen, S., Thermodynamic behaviour and the effect of temperature on the removal of dyes from aqueous solution using modified diatomite: A kinetic study, *J. Colloid Interface Sci.* **2005**, *287*, 6-13, DOI: 10.1016/j.jcis.2005.02.002.

[41] Krall, S. M.; Mc Feeters, R. F., Pectin hydrolysis: Effect of temperature, degree of methylation, pH, and calcium on hydrolysis rates, *J. Agric. Food Chem.* **1998**, *46*, 1311-15, DOI: 10.1021/jf970473y.

[42] Mendham, J.; Denny, R. C.; Barnes, J. D.; Thomas, M., Vogel's textbook of quantitative chemical analysis, Harlow Pearson Education England, **2000**, Appendix 5.

[43] Oakenfull, D.; Fenwic, D. E., Hydrophobic interaction in aqueous organic mixed solvents, *J. Chem. Soc. Faraday Trans.* **1979**, *75*, 636-45, DOI: 10.1039/F19797500636.

[44] Gerasov, A. O.; Zyabrev, K. V.; Shandura, M. P.; Kovtun, Y. P., The structural criteria of hydrolytic stability in series of dioxaborine polymethine dyes, *Dyes Pigm.* **2011**, *89*, 76-85, DOI: 10.1016/j.dyepig.2010.09.007.

[45] Barclay, L. R.; Vinqvist, M. R.; Mukai, K.; Goto, H.; Hashimoto, Y.; Tokunaga, A., On the antioxidant mechanism of curcumin: Classical methods are needed to determine antioxidant mechanism and activity, *Org. Lett.* **2000**, *2*, 2841-43, DOI: 10.1021/ol000173t.

[46] Jayaprakasha, G. K.; Rao, L. J. M.; Sakariah, K. K., Antioxidant activities of curcumin, demethoxycurcumin and bisdemethoxycurcumin, *Food Chem.* **2006**, *98*, 720-24, DOI: 10.1016/j.foodchem.2005.06.037.

[47] John, J.; Sudha, D. R.; Balachandran, S.; Babu, K. V. D., Synthesis, spectral characterization and thermal analysis of rubrocurcumin and its analogues, *J. Therm. Anal. Calorim.* **2017**, *130*, 2301-14, DOI: 10.1007/s10973-017-6582-z.

[48] Somparn, P.; Phisalaphong, C.; Nakornchai, S.; Unchern, S.; Morales, N. P., Comparative antioxidant activities of curcumin and its demethoxy and hydrogenated derivatives, *Biol. Pharm. Bull.* **2007**, *30*, 74-78, DOI: 10.1248/bpb.30.74.

[49] Bentley, T. W.; Carter, G. E., The SN2-SN1 spectrum. 4. The SN2 (intermediate) mechanism for solvolyses of tert-butyl chloride: a revised Y scale of solvent ionizing power based on solvolyses of 1-adamantyl chloride, *J. Am. Chem. Soc.* **1982**, *104*, 5741-47, DOI: 10.1021/ja00385a031.

[50] Fainberg, A. H.; Winstein, S., Correlation of solvolysis rates. III. t-butyl chloride in a wide range of solvent mixtures, *J. Am. Chem. Soc.* **1956**, *78*, 2770-77, DOI: 10.1021/ja01593a033.

[51] Bentley, T. W.; Koo, I. S.; Norman, S. J., Distinguishing between solvation effects and mechanistic changes. Effects due to differences in solvation of aromatic rings and alkyl groups, *J. Org. Chem.* **1991**, *56*, 1604-09, DOI: 10.1021/jo00004a048.

[52] Bunton, C. A.; Mhala, M. M.; Moffatt, J. R., Solvolysis of diphenylmethyl chloride and solvent nucleophilicity, *J. Org. Chem.* **1984**, *49*, 3639-41, DOI: 10.1021/jo00193a037.

[53] Ryu, Z. H.; Ju, C. S.; Sung, D. D.; Sung, N. C.; Bentley, T. W., Interpretation of dispersion phenomena in Grunwald-Winstein correlation for solvolyses of naphthoyl chloride, *Bull. Korean Chem. Soc.* **2002**, *23*, 123-31, DOI: 10.5012/bkcs.2002.23.1.123.

[54] Litwinienko, G.; Ingold, K. U., Abnormal solvent effects on hydrogen atom abstraction. 2. Resolution of the curcumin antioxidant controversy. The role of sequential proton loss electron transfer, *J. Org. Chem.* **2004**, *69*, 5888-96, DOI: 10.1021/jo049254j.

[55] Litwinienko, G.; Ingold, K. U., Abnormal solvent effects on hydrogen atom abstraction. 3. Novel kinetics in sequential proton loss electron transfer chemistry, *J. Org. Chem.* **2005**, *70*, 8982-90, DOI: 10.1021/jo051474p.

[56] Koh, H. J.; Kang, S. J., A kinetic study on solvolysis of 9-fluorenylmethyl chloroformate, *Bull. Korean Chem. Soc.* **2011**, *32*, 3799-3801, DOI: 10.5012/bkcs.2011.32.10.3799.

[57] Krajewska, B.; van Eldik, R.; Brindell, M., Temperature- and pressure-dependent stopped-flow kinetic studies of jack bean urease. Implications for the catalytic mechanism, *J. Biol. Inorg. Chem.* **2012**, *17*, 1123-34, DOI: 10.1007/s00775-012-0926-8.

[58] Gupta, V. K., Thermodynamic and related studies for the oxidation of sulpha drugs by the peroxydisulphate ion, *Thermochim Acta*. **1983**, *69*, 389-96, DOI: 0040-6031(83)80346-3.

[59] Gupta, V. K.; Pal, S.; Kumar, A.; Gupta, R.; Jain, N., Thermodynamic and related studies of the oxidation of *p*-aminobenzoic acid, sulphanilic acid and anthranilic acid by periodate, *Thermochim Acta*. **1989**, *140*, 197-202, DOI: 10.1016/0040-6031(89)87299-5.

[60] Pan, A.; Biswas, T.; Rakshit, A. K.; Moulik, S. P., Enthalpy-Entropy Compensation (EEC) effect: A revisit, *J. Phys. Chem. B*. **2015**, *119*, 15876-884, DOI: 10.1021/acs.jpcb.5b09925.

[61] Liu, L.; Guo, Q. -X., Isokinetic relationship, isoequilibrium relationship, and enthalpy-entropy compensation, *Chem. Rev.* **2001**, *101*, 673-95, DOI: 10.1021/cr990416z.

[62] Karunakaran, C.; Chidambaranathan, V., Linear free energy relationships near isokinetic temperature. Oxidation of organic sulfides with nicotinium dichromate, *Croat. Chim. Acta*. **2001**, *74*, 51-59, DOI: https://hrcak.srce.hr/131766.

[63] Kose, D. A.; Zumreoglu-Karan, B., Mixed-ligand complexes of boric acid with organic biomolecules, *Chem. Papers*. **2012**, *66*, 54-60, DOI: 10.2478/s11696-011-0108-0.

[64] Michael, A. B.; Catherine, C. B., Varma, A., 11B NMR study of zwitterionic and cationic monoborate complexes with cationic 1,2-diol ligands, *Polyhedron*. **2008**, *27*, 2226-30, DOI: 10.1016/j.poly.2008.04.007.

[65] Koji, I.; kira, N.; Kimiko, U.; Hideaki, I.; Kazuo, S., Kinetic study of boric acid-borate interchange in aqueous solution by 11B NMR spectroscopy, *Inorg. Chem.* **1994**, *33*, 3811-16, DOI: 10.1021/ic00095a026.

[66] Shao, C.; Matsuoka, S.; Miyazaki, Y.; Yoshimura, K.; Suzuki, T. M.; Tanaka, D. A. P., Equilibrium and kinetic studies on the complexation of boric acid with chromotropic acid, *J. Chem. Soc. Dalton Trans*. **2000**, *17*, 3136-42, DOI: 10.1039/B004399K.